

The role of lead component in second-harmonic generation in lead silica by electron-beam irradiation

Mingxin Qiu, F. Pi, and G. Orriols

Citation: *Applied Physics Letters* **73**, 3040 (1998); doi: 10.1063/1.122665

View online: <http://dx.doi.org/10.1063/1.122665>

View Table of Contents: <http://scitation.aip.org/content/aip/journal/apl/73/21?ver=pdfcov>

Published by the [AIP Publishing](#)

Instruments for advanced science

Gas Analysis



- dynamic measurement of reaction gas streams
- catalysis and thermal analysis
- molecular beam studies
- dissolved species probes
- fermentation, environmental and ecological studies

Surface Science



- UHV TPD
- SIMS
- end point detection in ion beam etch
- elemental imaging - surface mapping

Plasma Diagnostics



- plasma source characterization
- etch and deposition process
- reaction kinetic studies
- analysis of neutral and radical species

Vacuum Analysis



- partial pressure measurement and control of process gases
- reactive sputter process control
- vacuum diagnostics
- vacuum coating process monitoring

contact Hiden Analytical for further details

HIDEN
ANALYTICAL

info@hideninc.com
www.HidenAnalytical.com

CLICK to view our product catalogue 

The role of lead component in second-harmonic generation in lead silica by electron-beam irradiation

Mingxin Qiu^{a)}

Department of Electronics, Kyushu Institute of Technology, 1-1 Sensui-cho, Tobata-ku, 804 Kitakyushu, Japan

F. Pi and G. Orriols

Departament de Física, Universitat Autònoma de Barcelona, 08193 Bellaterra (Barcelona), Spain

(Received 24 February 1998; accepted for publication 28 September 1998)

It is found that the second-order nonlinearity induced in lead silica by electron-beam irradiation increases linearly with the lead percentage of the glass and a value of 4 pm/V has been estimated for ZF₇ lead silica. The electrostatic field created under the glass surface increases with the lead percentage, which can be explained by the theory of stopping collisions of fast electrons. The layer depth is found proportional to the inverse square root of the lead percentage. The accumulative effect of electron irradiation for inducing the nonlinearity appears limited by the breakdown threshold in the charged layer. An optimum total electron charge per unit of scanned area of 0.29 C/m² has been determined for SF₂ glass. Nonlinearity layer depths of 1.9–4.1 μm have been estimated by chemical etching for different lead silica and electron voltages, and the coefficients of the Bohr–Bethe penetration formula have been determined for SF₂ glass. © 1998 American Institute of Physics. [S0003-6951(98)04047-9]

Glass is a centrosymmetric material and has therefore no second-order susceptibility, $\chi^{(2)}$. However, a variety of centrosymmetry breaking procedures have been demonstrated in the last years and $\chi^{(2)}$ values as large as 1 pm/V have been achieved in the surface of pure silica by thermal poling under an applied electric field¹ and in the surface of a lead silica plate irradiated with an electron beam.²

Both the thermal poling^{3–8} and electron irradiation techniques⁹ lead to $\chi^{(2)}$ values of the same order in a thin layer beneath the glass surface. Nevertheless, Kazansky *et al.*⁹ have shown that the electron-beam irradiation does not work on pure silica but erases the second-order nonlinearity in thermally poled silica. The same authors observed the absence of second-harmonic (SH) signal in poled lead silica samples with unspecified Pb concentration. This motivated us to investigate the role of the lead component in both $\chi^{(2)}$ -inducing techniques and this letter presents results concerning with second-harmonic generation by electron-beam irradiation on a variety of lead silica glasses. We have found that the SH signal by electron implantation increases linearly with the lead concentration. On the other hand, SH generation has been also observed in thermally poled lead silica with high Pb concentration and in this case the SH signal increases exponentially with the Pb concentration.¹⁰

We used different kinds of commercial lead silica glasses, F₂, SF₂, SF₁₁, and ZF₇, in which the weight concentration of PbO is 47%, 51%, 61%, and 71%, respectively, and other components as listed in Table I. The 2-cm-diam 1-mm-thick samples, polished on both sides, were irradiated by an electron beam in a scanning electron microscope. Three scanning modes were alternatively used: TV mode (0.017 s/frame with 255 scanning lines), SL3 mode (20 s/

frame with 1000 scanning lines), and PH mode (160 s/frame with 2000 scanning lines). The scanned area was 5 × 3.7 mm² in the center of the sample and the line spacing for the three modes was 14.5, 3.7, and 1.8 μm, respectively.

After irradiation the samples were tested for evidence of SH generation. A Q-switched Nd:yttrium aluminum garnet (YAG) laser providing 0.4 mJ, 6 ns pulses of 1.064 μm radiation was focused onto the electron-beam scanned area of the sample in similar conditions as in Ref. 1. The focus spot was of 40 μm in diameter and it covered a certain number of scanning lines (from two or three in the TV mode to more than ten in the other modes). The SH signal from the treated lead silica samples was calibrated by comparing with the signal obtained from a piece of crystalline quartz under similar light irradiation conditions. A $\chi^{(2)}$ value of about 4 pm/V was estimated for a ZF₇ sample scanned at 6 nA and 30 kV for 15 min in SL3 mode or, equivalently, with a total electron charge (TEC) per unit of scanned area of 0.291 C/m². The phase matching factor has not been considered by assuming an effective layer depth of 2 μm, much less than the coherence distance of 7 μm.

As shown in Fig. 1, the SH signal increases linearly with

TABLE I. Composition in percentage of the lead silica glasses used in the work.

	Lead silica glasses			
	F ₂	SF ₂	SF ₁₁	ZF ₇
PbO	46.65	51.18	61.23	70.93
SiO ₂	46.44	41.32	31.19	27.27
NaO ₂	0.71	...	0.45	0.5
K ₂ O	5.46	7.0	5.932	1.0
As ₂ O ₃	0.05	0.05	1.0	0.3
Sb ₂ O ₃	0.25	...	0.2	...

^{a)}Electronic mail: qiu@elcs.kyutech.ac.jp

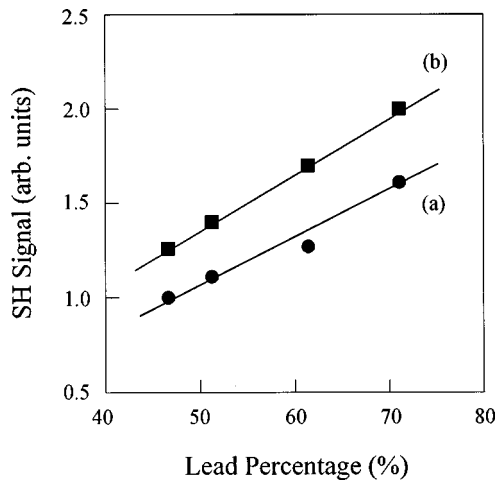


FIG. 1. SH signal obtained from lead silica glasses of different lead concentration. The electron beam irradiation was at 6 nA and 30 kV in SL3 mode, and for 5 min (a) or 15 min (b). The total electric charge per unit of scanned area was 0.097 (a) and 0.291 C/m² (b).

the lead percentage. The samples were irradiated with 6 nA at 30 kV in SL3 mode, either during 5 min, line (a), or 15 min, line (b). These two irradiations correspond to a TEC of 0.097 and 0.291 C/m², respectively. The slope of line (b) is larger than that of line (a). The increase of three times of the TEC produces increases of about 30%–40% in the SH signal only. The SH signal from ZF₇ is about 60% larger than that from F₂. Similar results were obtained for the different scanning modes so that the density of scanning lines is not significant. The SH signal depends on the lead percentage in the lead silica glass and on the TEC of the electron irradiation.

The role of lead can be understood in a twofold way: the permanence of charges and the enhancement of the ionization rate by electron collisions. According to the results of Ref. 2, there exists a pair of positive and negative charged layers below the glass surface and the negative layer locates deeper than the positive one. A strong space-charge electrostatic field is created and, acting on the third-order susceptibility induces the $\chi^{(2)}$ nonlinearity in the layered structure. The presence of lead may aid in establishing the positive layer by the ionization collisions of electrons with lead oxide radicals, while the electrons stop deeper and build the negative layer there. On the other hand, during the stopping collision of fast electrons on glass, most of the energy of the electrons is exhausted in exciting substrate molecules and only a small part of it contributes to the ionization collision.¹¹ The ionization rate per cm is

$$S_0 = \frac{2\pi N e^4}{m v^2} \sum_{nl} \frac{c_{nl} Z_{nl}}{-E_{nl}} \log \frac{2 m v^2}{C_{nl}}, \quad (1)$$

where N is the atomic density on the target, $m v^2/2$ is the kinetic energy of electron, e is the electron charge, n and l are the shell quantum numbers, Z_{nl} is the electron number in the shell, $-E_{nl}$ is the electric strength in the shell, C_{nl} is the quantity characterizing the energy of the shell, and c_{nl} is an integral matrix element proportional to the square of effective nuclear charges acting on the nl shell electrons. Hence, the ionization rate is proportional to the square of effective nuclear charges and so the ionization cross section of lead is much larger than that of silicon. The ionized charge per unit

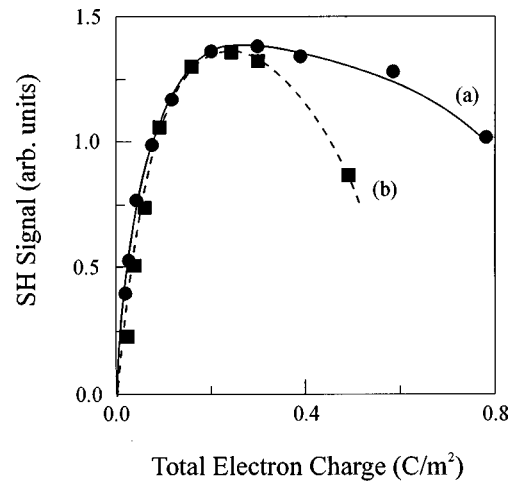


FIG. 2. SH signal in SF₂ samples as a function of the total electric charge by changing either the irradiation time with a fixed current of 6 nA, curve (a), or the beam current with a fixed time of 15 min, curve (b). The electron-beam scanning was at 30 kV in SL3 mode.

area is proportional to the lead concentration, N , because the effective nuclear charges of other elements are much less. Thus, $\chi^{(2)} \propto 3 \chi^{(3)} E \propto N \propto r$, where $\chi^{(3)}$ is the third-order susceptibility of lead silica, E the electrostatic field and r the lead percentage. Since the SH signal may be assumed proportional to $(\chi^{(2)} L)^2$, where L is the depth of the nonlinear layer, and the experimental results indicate a linear growing with r , we then conclude that $L \propto r^{-1/2}$.

Figure 2 shows the SH signal in SF₂ samples as a function of the irradiated TEC values by changing either the irradiation time with a fixed current of 6 nA, curve (a), or the beam current with a fixed time of 15 min, curve (b). The maximum of curve (a) at 0.29 C/m² corresponds to 15 min so that both curves would be coincident in that point but different samples were used for the measurements. The curves overlap closely for low TEC values, but curve (b) drops quicker than curve (a) at the other side of the maximum. Electric breakdown occurs in the space-charged layer for TEC values larger than the optimum and the inner field becomes weakened. The inhomogeneous distribution of charges when scanning at high electron currents probably explains the stronger breakdown effects in curve (b). Similar behavior was observed in other lead silica glasses.

We analyzed the depth profile of the nonlinearity by applying differential chemical etching with a very dilute HF solution (0.5 wt. %) and measuring the residual SH signal. The etched depths were determined with a Michelson inter-

TABLE II. Etching results in SF₂ samples irradiated in the SL3 scanning mode at 6 nA for 5 min (TEC) of 0.097 C/m².

30 kV	Etched depth (μm)			
	0	2.5	4.5	5.5
SH signal (arb. units)	760	680	280	120
25 kV	Etched depth (μm)			
	0	2.3	4.3	5.0
SH signal (arb. units)	725	610	90	...
20 kV	Etched depth (μm)			
	0	1.4	2.7	4.0
SH signal (arb. units)	550	400	50	...

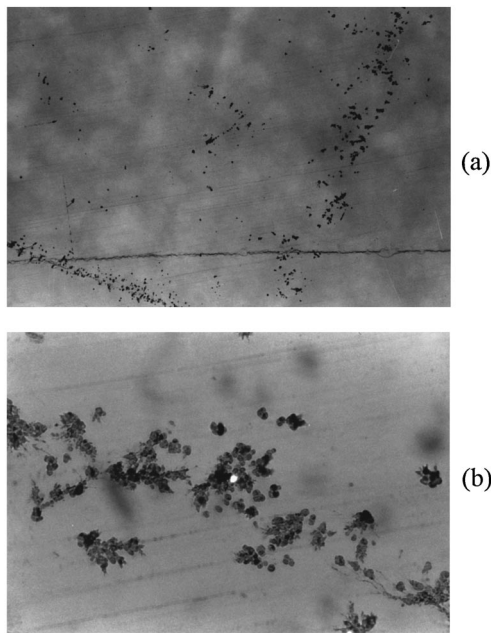


FIG. 3. (a) Microscopic view covering $2.7 \text{ mm} \times 1.8 \text{ mm}$ of the etched surface of a SF_2 sample. The electron-beam irradiation was at 6 nA and 30 kV, for 5 min in the SL3 mode. The horizontal line near the bottom denotes the space-selective etching in-between 2 and 7 min etching times. The black spots are deep holes due to fast etching and appear distributed along the edges of the scanned area. (b) Enlarged view of the scanned area edge covering $0.69 \text{ mm} \times 0.46 \text{ mm}$.

ferometer microscope. Table II presents some results for SF_2 samples irradiated in SL3 mode with 6 nA and different electron voltages. By considering the etching depths required to halve the SH signal, we estimate the depth of the nonlinear layer to be $4.1 \mu\text{m}$ for 30 kV, $3.1 \mu\text{m}$ for 25 kV, and $1.9 \mu\text{m}$ for 20 kV. The penetration of electrons in the lead silica can be calculated from the Bohr–Bethe formula^{12,13}

$$d = CE_0^\alpha, \quad (2)$$

where d is the penetration in μm , E_0 is the electron energy in keV, α and C are constants depending on the material and from the etching data are estimated to be $\alpha=0.46$ and $C=0.57$ for the SF_2 glass. Table II does not give a linear relation between the SH signal and the electron voltage. If the scanning time is changed to 15 min at 6 nA, 30 kV in SL3 mode, the charged depth of SF_2 becomes $2.2 \mu\text{m}$. The

depths in scanned ZF_7 glass are $2 \mu\text{m}$ for 15 min and $3.5 \mu\text{m}$ for 5 min, at 6 nA and 30 kV in SL3 mode. The layer depth basically satisfies the inverse square root relation, $L \propto r^{-1/2}$.

Figure 3(a) shows a microscopic view of the scanning pattern after etching. The horizontal straight line denotes an etching step and the black dots denote deep holes formed on the edge of the scanned area. Such holes appear quickly during the first etching step and may be associated with accumulation of charges induced by the electron-beam scanning dynamics.

In conclusion, we found that the second-order nonlinearity induced in lead silica by electron beam irradiation increases linearly with the lead percentage of the glass. This can be explained from the theory of stopping collision of fast electrons, showing that the ionization rate is proportional to the lead percentage, r , and the depth of the induced charge distribution is proportional to $r^{-1/2}$. The $\chi^{(2)}$ value of 4 pm/V obtained in ZF_7 glass irradiated with 0.29 C/m^2 is about four times that found in poled pure silica. The depth of the charged layer has been estimated by chemical etching and the values of $1.9\text{--}4.1 \mu\text{m}$ have been obtained for different electron voltages in different lead silica glasses.

¹R. A. Myers, N. Mukherjee, and S. R. J. Brueck, *Opt. Lett.* **16**, 1732 (1991).

²P. G. Kazansky, A. Kamal, and P. St. J. Russell, *Opt. Lett.* **18**, 693 (1993).

³N. Mukherjee, R. A. Myers, and S. R. J. Brueck, *J. Opt. Soc. Am. B* **11**, 665 (1994).

⁴H. Takebe, P. G. Kazansky, and P. St. J. Russell, *Opt. Lett.* **21**, 468 (1996).

⁵H. Nasu, H. Okamoto, K. Kurachi, J. Matsuoka, K. Kamiya, A. Moto, and H. Hosono, *J. Opt. Soc. Am. B* **12**, 644 (1995).

⁶L. J. Henry, A. D. Devilbiss, and T. E. Tsai, *J. Opt. Soc. Am. B* **12**, 2037 (1995).

⁷A. Okada, K. Ishii, K. Mito, and K. Sasaki, *Appl. Phys. Lett.* **60**, 2853 (1992).

⁸A. Le Calvez, E. Freysz, and A. Ducasse, *Opt. Lett.* **22**, 1547 (1997).

⁹P. G. Kazansky, A. Kamal, and P. St. J. Russell, *Opt. Lett.* **18**, 1141 (1993).

¹⁰M. Qiu, T. Mizunami, H. Koya, F. Pi, and G. Orriols, in *Proceedings of Nonlinear Optics: Materials, Fundamentals, and Applications* (IEEE, Piscataway, NJ, 1998), p. 370.

¹¹N. F. Mott and H. S. W. Massey, *The Theory of Atomic Collisions* (Oxford University Press, London, 1965), p. 519.

¹²T. E. Everhart and P. H. Hoff, *J. Appl. Phys.* **42**, 5837 (1971).

¹³D. Barbier, M. Green, and S. J. Madden, *J. Lightwave Technol.* **9**, 715 (1991).